Journal of Catalysis 260 (2008) 371–379

Contents lists available at ScienceDirect

Journal of Catalysis

www.elsevier.com/locate/jcat

IR spectral evidence of aldol condensation: Acetaldehyde adsorption over TiO_2 surface

Manishwar Singh [a,1], Nanjia Zhou [a], Dilip K. Paul [a,*], Kenneth J. Klabunde [b]

[a] Pittsburg State University, Pittsburg, KS 66762, USA
[b] Kansas State University, Manhattan, KS 66506, USA

ARTICLE INFO

Article history:
Received 29 March 2008
Revised 27 June 2008
Accepted 26 July 2008
Available online 1 November 2008

Keywords:
3-Hydroxybutanal
Aldol condensation
Acetaldehyde
FT-IR
TiO_2
Nanoparticles

ABSTRACT

The adsorption of acetaldehyde on particulate TiO_2 surfaces has been studied at 233 K by FT-IR spectroscopy using a specially designed IR cell. It has been found that acetaldehyde initially adsorbs onto the surface through hydrogen bonding and Lewis acid sites. As the temperature is raised to 251 K, the spectroscopic evidence of formation of 3-hydroxybutanal surface intermediate is observed during aldol condensation reaction. The presence of this transient species has been characterized by the infrared features at 3185 cm^{-1}—ν(OH), 1334 cm^{-1}—δ(CH), 1273 cm^{-1}—δ(COH), and 1105 cm^{-1}—ν(C–C) and δ(COH). The assignments of all surface species are confirmed by adsorbing pure 3-hydroxybutanal and 2-butenal on TiO_2 surface. A reaction mechanism consistent with the detectable surface intermediates is proposed.

1. Introduction

Titanium dioxide is a well known semiconductor oxide with a band gap of ~3.2 eV [1]. It is responsible for catalyzing a variety of organic reactions including decomposition of organic pollutants in aqueous solution or in air and as a self cleaning smart material [2,3]. It has the highest photo-catalytic activity among all oxide semiconductors [3,4]. The ability of TiO_2 and TiO_2 based photo-catalysts to completely destroy of organic compounds during photochemical oxidation has attracted considerable attention, and thus is useful for environmental remediation [5]. The phenomenon of the discovery of photo-induced water splitting at TiO_2 electrodes has revolutionized the area of TiO_2-mediated heterogeneous photo-catalysis [6]. Many organic reactions on oxides surfaces are known to be catalyzed by the surface acid and base sites. Besides the semiconductor properties, its acid base sites on the surface play a key role in catalyzing several reactions including an important class of reaction—the aldol condensation.

Aldol condensation is important in synthetic organic chemistry, because it leads to the formation of a carbon–carbon bond. Extensive works have been done on the reaction of aldehydes with different metal oxides system, and over different types of zeolites [7–11]. In all those studies, the formation of aldol has been reported but there was no direct spectroscopic evidence of the formation of the reaction intermediate [7,8,12]. Herein, we report spectral evidence of the formation of 3-hydroxybutanal (aldol) over TiO_2 as an intermediate during the conversion of acetaldehyde to 2-butenal.

Recently several studies have been reported on the reaction of acetaldehyde on high area metal oxide surfaces at above room temperature. Idriss et al. [7] in their study on single crystal and polycrystalline TiO_2 surfaces using TPD and XPS, reported that when acetaldehyde adsorbs on TiO_2, lattice oxygen acts as a base to abstract a proton from the α-carbon position of the acetaldehyde to form $-CH_2CHO$, a nucleophile, which can attack the electrophilic carbonyl carbon of another acetaldehyde to form an adsorbed aldol which upon dehydration produces 2-butenal. Idriss and Barteau [8] found that aldol condensation of acetaldehyde to 2-butenal and 2-butenol is favored on oxidized surfaces of TiO_2 which contains more surface oxide anions, whereas reduced surfaces facilitate the formation of 2-butene, the product of reductive coupling. Swift et al. [13] studied the liquid phase reaction of n-butyraldehyde at 383 K over γ-Al_2O_3 and alkaline earth oxides, forming 2-ethyl-hexenal (ethyl propyl acrolein) which takes place on basic sites, but they did not provide any evidence of an aldol intermediate in the study. In another study by using IR spectroscopy and temperature programmed desorption, Idriss and co-workers [14] observed several reactions of acetaldehyde which include oxidation, reduction and C–C bond formation on the surface of CeO_2 and CeO_2 supported catalysts. It is important to mention here that these reactions were carried out by these groups at or above room temperature.

---

[*] Corresponding author. Fax: +1 620 235 4003.
E-mail address: dpaul@pittstate.edu (D.K. Paul).

[1] Currently pursuing Ph.D. at Chemistry Department of the University of Kansas.

0021-9517/$ – see front matter © 2008 Elsevier Inc. All rights reserved.
doi:10.1016/j.jcat.2008.07.020

In this study acetaldehyde was adsorbed at 233 K, and the aldol condensation reaction was spectroscopically monitored in the temperature range of 233 to 273 K. The formation and decomposition of aldol was observed on the surface initially at 251 K and it is optimized at ∼255 K. *The importance of the present study lies in the fact that it has been carried out at low temperature to carefully observe the evolution of spectral features corresponding to aldol and other products. To the best of our knowledge, no IR study has been reported providing spectroscopic evidence of formation of* 3*-hydroxybutanal intermediate during the condensation reaction of acetaldehyde*.

2. Experimental and methods

2.1. Experimental

TiO_2 used in the experiment was purchased from Degussa "Titandioxid P25." The product has the surface area of 50 m^2/g and crystallite size of 21 nm.

Approximately 5–6 mg powder sample was pressed hydraulically (12,000 lb/in^2) on a square inch Tungsten mesh (0.0508 mm thick, with 0.22 mm^2 holes) at a circular spot of 7 mm in diameter (1.3–1.9 mg/cm^2) [15]. The upper third position on the grid was kept empty and was used as background to collect the sample spectrum. The grid used in this experiment was ∼80% transparent so that the incident IR beam could pass through the sample efficiently. The sample containing grid was then placed at the center of UHV stainless steel cell and was held by nickel clamps along the grid edges [16]. A chromel/constantan wire was spot welded on the middle of the top edge of the grid which in turn was welded to the thermocouple power feed through to measure the temperature. The sample can be heated by resistive heating using power supply/temperature programmer up to 1500 K, and it can also be cooled down to 100 K with conductive cooling using liquid nitrogen. The IR cell was then mounted on a computer controlled translation system (Newport Corporation), capable of moving the cell to ±1 µm accuracy in both horizontal and vertical directions. The total volume of the IR cell used in this experiment is 317 mL. The IR cell was connected to an ultra high vacuum gas manifold. The system can routinely attain a base pressure of 1×10^{-8} Torr by pumping through 60 L/s turbomolecular pump backed by an oil free diaphragm pump. The KBr cell windows were mounted on concentric Viton O-rings which are differentially pumped to prevent any air leakage.

Infrared spectra were obtained with a dry CO_2 free air purged Mattson Research Series I FTIR spectrometer, and was equipped with a narrow band HgCdTe detector operating at 77 K or liquid nitrogen temperature. All IR spectra were collected by co-adding 300 scans at a resolution of 4 cm^{-1}. Acetaldehyde (99%), 2-butenal (99%), and 3-hydroxybutanal (99%) used in this work were purchased from Sigma Aldrich. These liquids were stored in separate cleaned and pre-dried glass bulbs and purified by five freeze–pump–thaw cycles using a vacuum manifold. Oxygen used in the experiment was obtained from Matheson and was 99.999% pure.

Tungsten mesh containing the sample was placed in the UHV stainless steel cell, was allowed to evacuate for ∼6 h. Thereafter the temperature was raised to 473 K and allowed to evacuate overnight to get rid of any water present in the sample. The sample temperature was then raised gradually to 823 K for calcination using 20 Torr oxygen. After two cycles of calcinations, the sample temperature was raised to 873 K for 30 min before cooling down to the temperature of adsorption which was usually 173 K. Adsorption of acetaldehyde was carried out at this temperature and the IR data were collected as needed.

2.2. Observed and calculated IR frequency for different modes of 3-hydroxybutanal

No reported IR data of 3-hydroxybutanal are available in literature and thus infrared spectrum for 3-hydroxybutanal was obtained at 173 K. These spectral data were compared with adsorption data and are outlined in Table 1. The experimental data were compared with calculated data (Gaussian 03 [17,18]) to confirm the different vibrational modes for 3-hydroxybutanal. All calculations have been carried out by Gaussian 03 software using B3LYP functional calculation method and 6-311G** as a basis set. A smaller basis set in DFT theory is sufficient as it does not have to describe the correlation orbital. All the calculated IR frequencies by using 6-311G** need to be corrected by an appropriate correction factor to compare with the observed result. All the errors in calculations are largely systematic and can be corrected by using an empirical scaling factor [19]. Pulay and Meyer [20] used a correction factor for diminishing the diagonal stretching force constants by 10% and the diagonal bending constants by 20%, leaving the coupling constants unchanged for IR frequencies for ethane, ethylene, and acetylene. The best scale factor for all the force constant to optimize a single reasonable force constants is close to 0.9 [21–25]. In order to scale the calculated IR frequencies of 3-hydroxybutanal, a single 0.9 scaling factor is used to compare the observed result. The observed values matched with the calculated values within a permissible range.

Table 1
Vibrational peak assignments of gas phase and adsorbed 2-butenal and 3-hydroxybutanal.

2-Butenal				3-Hydroxybutanal				
					173 K			251–257 K
Mode	Gas [38]	2-Butenal/TiO_2 [12,33]	2-Butenal/TiO_2 [a]	Mode	Gas phase aldol [a]	Aldol/TiO_2 [a]	Calculated, 6311G** Scaled *0.9	Acetaldehyde/TiO_2 [a,b]
υ(C=C–H)	3058	3038/3036	3017	υ(OH)	3305	3237	3396	3185
$\upsilon(CH)sp^2$	2995	–	2977	$\upsilon_{as}(CH_3)$	2974	2970	2799	2968
$\upsilon_{as}(CH_3)$	2963	2954/2950	2968	$\upsilon_s(CH_3)$	2946	2941	2731	2941
$\upsilon_s(CH_3)$	2938	2920/2905	2941/2931	υ(CH)	2848	2857	2728	2857
Resonance	–	2845/2830	2857	υ(C=O)	1664	1682	1613	1656
υ(CH)	2805/2738	2745/2740	2822	$\delta_{as}(CH_3)$	1439	1445	1352	–
υ(C=O)	1720	1686/1656	1656	$\delta_s(CH_3)$	1432	1426	1334	–
$\delta_{as}(CH_3)$	1455	–	1442	δ(CH)	1322	1320	1286	1334
$\delta_s(CH_3)$	1391	1394/1406	1376	δ(C–OH)	1255	1257	1196	1273
υ(C–C)	1147	1165/1152	1148	υ(C–C)	1172	1164	1196	–
				δ(COH), υ(C–C)	1091	1105	1016	1105

[a] This work.

[b] Vibrational assignments for 3-hydroxybutanal formed during warm-up of acetaldehyde/TiO_2.

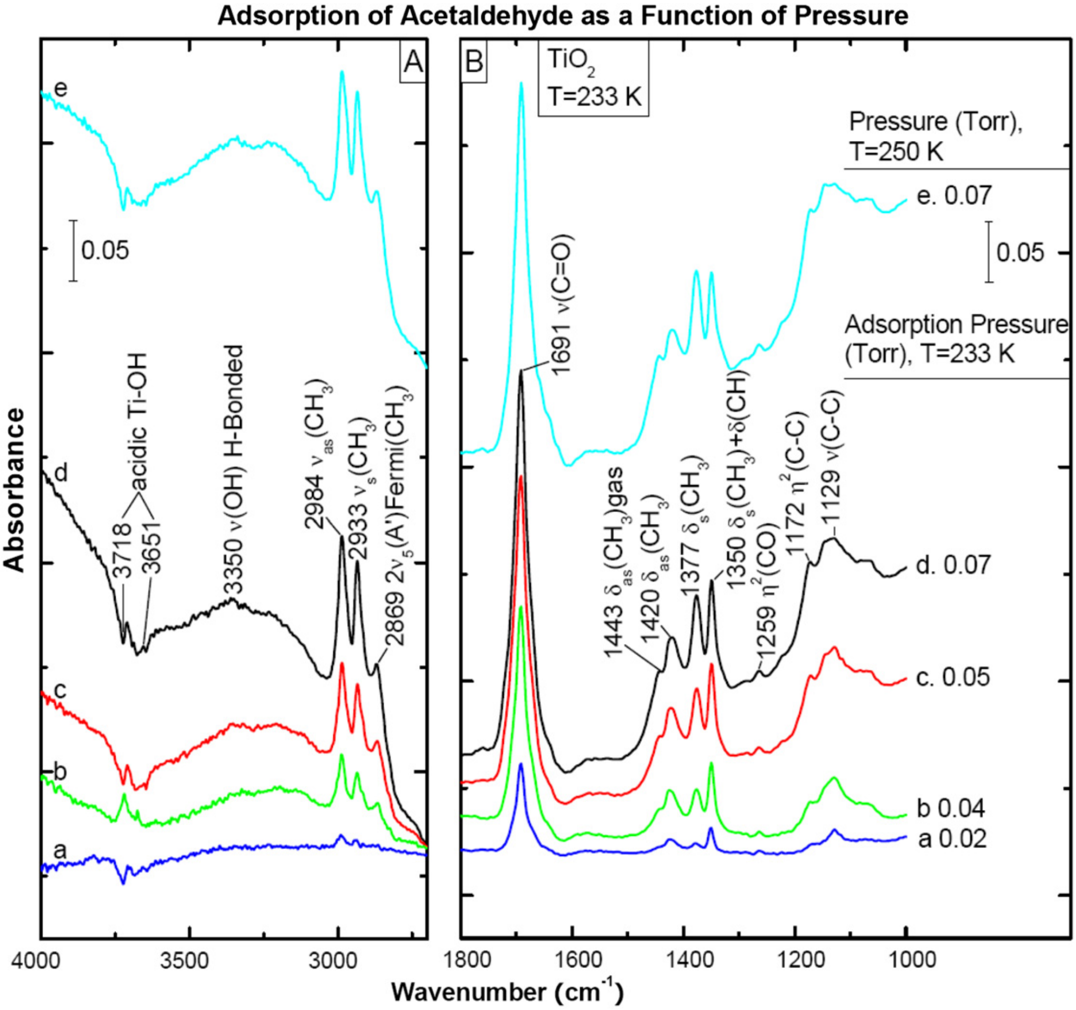

Fig. 1. Infrared spectra of acetaldehyde (CH_3CHO) adsorbed on TiO_2 surface as a function of coverage (spectra (a)–(d)) at 233 K. (a) 0.02 Torr; (b) 0.04 Torr; (c) 0.05 Torr; (d) 0.07 Torr; spectrum (e) warmed to 250 K.

3. Results and discussion

3.1. Low temperature acetaldehyde adsorption: Observation of H-bonding through surface –OH

Fig. 1 shows the infrared spectral development for sequential exposure of acetaldehyde vapor over TiO_2 at 233 K starting at 0.02 Torr. All spectra shown in Fig. 1 are ratioed to the blank TiO_2 surface spectrum collected at 233 K just prior to acetaldehyde exposure. As the surface is slowly exposed to acetaldehyde vapor with increasing pressure, the infrared spectral features (Figs. 1A and 1B, spectra (a)–(d)) developed in both CH–OH stretching (4000–2000 cm^{-1}) and bending regions (1800–1000 cm^{-1}) which gained/or decreased intensities gradually as a function of coverage. The peaks that gained intensities at the CH stretching regions were observed at 2984, 2933, and 2869 cm^{-1}, which can be assigned to $\nu_{as}(CH_3)$, $\nu_s(CH_3)$, and $2\nu_5(A')\nu_s(CH_3)$ modes, respectively, whereas the peak with negative intensity at $\sim$3700 cm^{-1} can be assigned to ν(OH) for Ti–OH. This assignment is consistent with the interpretation of Tsyganenko et al. [26–28] where they found the ν(OH) peak at 3718 cm^{-1} assignable for hydroxyl groups attached to tetrahedrally or octahedrally coordinated Ti^{4+} sites on TiO_2. In another study over alumina surfaces, Knözinger and Ratnasamy [29] reported that the band developed at $\sim$3722 cm^{-1} is due to ν(OH) of hydroxyl groups attached to coordinatively unsaturated Al^{3+} sites. It is important to note that the Brönsted acid strength and H-bond strength of a given OH-group increase with the co-ordination number of a given oxide [30]. In addition, the growth of a substantially prominent broad peak centered at $\sim$3350 cm^{-1} is clearly observed as the coverage of acetaldehyde is increased (Fig. 1A, spectra (a)–(d)).

Several spectral features developed during the course of acetaldehyde (Fig. 1B) exposure in the fingerprint region 1800–1000 cm^{-1} which include the peaks at 1691 cm^{-1} ν(C=O), 1443 cm^{-1} $\delta_{as}(CH_3)$, 1377 cm^{-1} $\delta_s(CH_3)$, 1350 cm^{-1} $\delta_s(CH_3) + \delta(CH)$ and peaks at 1259, 1172, and 1129 cm^{-1} can be assigned to η^2(CO), η^2(C–C), and ν(C–C) modes of acetaldehyde, respectively [12,14,31–33]. The frequencies of all the spectral features except the ν(C=O) mode (1722 vs 1691 cm^{-1}) at 233 K adsorption are similar to the gas phase spectrum of acetaldehyde as shown in Table 2. This observation indicates that a fraction of acetaldehyde adsorbed on the surface probably through Lewis acid–base forces, by the interaction of the carbonyl group and coordinatively unsaturated Ti^{4+} ($>C=O \rightarrow Ti^{4+}$) [31].

As the surface is exposed to acetaldehyde vapor, the gradual decrease in intensities of ν(OH) modes at 3718 and $\sim$3700 cm^{-1} along with the growth of a broad band at 3350 cm^{-1} is indicative of H-bonding of free surface –OH groups with acetaldehyde, $Ti{=}OH\cdots OHCCH_3$ [34–36]. Thus a large fraction of acetaldehyde adsorbs onto the surface through H-bonding, although the amount depends on the number of –OH groups present.

Table 2
Vibrational assignment for gas phase and adsorbed acetaldehyde on TiO_2.

Peak assignment	Gas phase [37,38]	TiO_2, CeO_2 [12,14,31–33]	This work (233 K)
$\upsilon_{as}(CH_3)$	3003	2969	2984
$\upsilon_s(CH_3)$	2923	2918	2933
$2\upsilon_6A'$ Fermi	2840	2843	2869
$\upsilon(CH)_{ald}$	2716	2759	–
$\upsilon(C{=}O)$	1722	1718/1703	1691
$\delta_{as}(CH_3)$	1433	1422	1420/1443
$\delta_s(CH_3)$	1395	1391	1377
$\delta(CH)$	1352	1350	1350
$\eta^2(CH_3)$	–	1220	1259
$\eta^2(C–C)$	–	1175	1172
$2\upsilon_{10}A'$	–	1038	1060
$\upsilon(C–C)$	920	975	928
$\upsilon(C–O)$	867	885	876

Figs. 1A and 1B (e) show the spectrum taken upon warming the adsorbed acetaldehyde to 250 K. No apparent change in spectral behavior is noticed other than the enhanced decrease/increase in Ti–OH intensities (at ∼3700 and ∼3350 cm^{-1}) indicating an increasing number of adsorbed acetaldehyde molecules are involved in H-bonding. Thus, the surface reactions that can be identified within the temperature range of 233–250 K are mainly through coordination of acetaldehyde to Ti^{4+} sites and through H-bonding to surface –OH groups.

3.2. Temperature dependence of acetaldehyde adsorption: Aldol condensation—formation of 3-hydroxybutanal and 2-butenal

Figs. 2A and 2B indicate the infrared spectral data obtained at different temperatures starting at 251 K during warming of adsorbed acetaldehyde over TiO_2. The effect of temperatures below 251 K has been shown in Fig. 1. All the spectra shown in this Fig. 2 are obtained by subtracting spectrum collected at 250 K shown Figs. 1A and 1B (e). As can be seen in Fig. 1 (spectra (d) and (e)), there are no apparent changes in shape and intensity of infrared features for acetaldehyde adsorption at both 233 and 250 K, indicating that there is no detectable surface reaction other than H-bonding. The heat induced surface reaction was then monitored at 251 K for a period of 55 min while collecting IR data every 3 min, and then raised the temperature by an interval of 1 K again to 257 K. Thus at this slow excursion of temperature, the use of background obtained at 250 K provided us the key information about the surface intermediates to investigate the mechanism of reaction. However, only selected data at 251, 254, and 257 K were presented here for clarity purposes.

As the adsorbed acetaldehyde was slowly and carefully warmed to 251 K (Figs. 2A and 2B, spectra (a)–(c)) for a period of 3, 30 and 60 min, a change in intensities of infrared features is observed in both υ(C–H) and fingerprint (1800–1000 cm^{-1}) regions of the spectra. The bands at 2984 and 2933 cm^{-1} lose intensities while the gain in intensities is noted for the infrared features at 2968 and 2941 cm^{-1} (spectra (a)–(c) in Fig. 2A). These dramatic intensity changes are accompanied by an increased absorbance for peaks developed at 1656, 1642/1630, 1442, 1376, 1273, 1148, and 1105 cm^{-1} (Fig. 2B, spectra (a)–(c)) along with the decrease in absorbance for peaks at 1691, 1420, and 1352 cm^{-1}. The changes in spectral intensities described above were continued as the surface temperature was slowly raised to 254 K for a period of 40 min and then again to 257 K as shown in Figs. 2A and 2B, spectra (d)–(l).

The assignments of all infrared features responsible for the surfaces species developed or depleted are outlined in Table 3. The peaks at 2984 and 2933 cm^{-1} that lost intensities can be assigned to $\upsilon_{as}(CH_3)$ and $\upsilon_s(CH_3)$, respectively, for adsorbed CH_3CHO. The corresponding decrease in intensities of infrared peaks at 1691, 1420 and 1352 cm^{-1} can be attributed to $\upsilon(C{=}O)$, $\delta_{as}(CH_3)$, and a combination of $\delta(CH_3)$ and $\delta(CH)$ modes, respectively. This observation indicates that the gradual depletion of acetaldehyde surface species continued as the temperature was raised. Here the newly developed infrared features at 2977, 2968, 2941, and 2931 cm^{-1} can be assigned to $\upsilon(CH)$ modes of condensation products derived from surface reactions. The broad feature at 3185 cm^{-1} due to $\upsilon(OH)$ grew in intensity as the temperature was raised, indicative of the formation of surface species containing –OH groups [39]. In addition, a broad band appeared at ∼3400 cm^{-1} as a shoulder which can be assigned to $\upsilon(OH)$ of water that formed during the reaction. The identity of other spectral features mentioned above awaits further explanation once the corresponding fingerprint region is described in the next paragraph.

Table 3
Vibrational frequencies (cm^{-1}) for aldol condensation: Formation of 3-hydroxybutanal and 2-butenal.

	Depletion of acetaldehyde surface species	Formation of 3-hydroxybutanal and 2-butenal surface species
Peak assignment	Decreasing absorbance (cm^{-1})	Increasing absorbance (cm^{-1})
$\nu(OH)$	–	3185^b
$\upsilon(C{=}C–H)sp^2$	–	3017^c
$\upsilon(CH)sp^2$		2977^c
$\nu_{as}(CH_3)$	2984^a	$2968^{b,c}$
$\nu_s(CH_3)$	2933^a	$2941/2931^{a,b,c}$
$\upsilon(C{=}O)$	1691^a	1656^c
$\upsilon(C{=}C)$	–	1642^c, 1630^c
$\delta(CH_3)$	1420^a, 1352^a	$1442^{b,c}$, 1376^c
$\delta(CH)$aldol	–	1334^b
$\delta(C–OH)$	–	1273^b
$\upsilon(C–C)$	–	1148^c
$\delta(C–OH)$, $\upsilon(C–C)$	–	1105^b

[a] Acetaldehyde.
[b] 3-Hydroxybutanal.
[c] 2-Butenal.

The growth of the infrared features at 1656, 1642/1630, 1442, and 1376 cm^{-1} in the 1800–1000 cm^{-1} region can be assigned to $\upsilon(C{=}O)$, $\upsilon(C{=}C)$, $\delta_{as}(CH_3)$ and $\delta_s(CH_3)$ modes respectively, as identified in the last column of Table 3. This suggests that the possible surface species contains >C=O, –OH, and C=C functionalities that could be a possible mixture of aldol and 2-butenal (usual products of aldol condensation reaction). These assignments are based on elegant studies of adsorption of 2-butenal over TiO_2 (anatase and rutile) made by Rekoske and Barteau [12] where they assigned 1686/1656 and 1636/1602 cm^{-1} for $\upsilon(C{=}O)$ and $\upsilon(C{=}C)$, respectively. Recent separate studies also by Chang et al. [31] and Jesus and Zaera [40] for 2-butenal adsorption over $SrTiO_3$ and Pt(111) indicated the appearance of carbonyl stretching modes at 1667 and 1694 cm^{-1}, which is consistent with our assignment.

In addition to these infrared features, the weak bands that grew in intensity over time at 1334, 1273, and 1105 cm^{-1} which could be assigned to $\delta(CH)$, $\delta(C–OH)$, and overlapping of $\upsilon(C–C)$ and $\delta(C–OH)$ modes, respectively [41,42], indicate the presence of both of 3-hydroxybutanal and 2-butenal surface species. Barnes and Hallam [43] assigned the IR feature at 1240 cm^{-1} for the OH in-plane bending mode of ethanol in an argon matrix. Similarly, Green [44] observed the infrared feature for frozen isopropanol at 1256 cm^{-1}, which is mainly due to C–O–H in plane bending. The IR studies of CH_3CH_2OH/TiO_2 performed by Yu and Chuang [32] identified the 1274 cm^{-1} band as $\delta(OH)$ mode of adsorbed ethanol, whereas on CeO_2, a similar feature at 1292 cm^{-1} has been assigned for molecularly adsorbed ethanol [41].

The decrease in intensities of the peaks at 1352 and 1420 cm^{-1} lead to the formation of 1334 cm^{-1} which can be assigned for $\delta(CH)$ aldol species formed on the surface. Chang et al. [31], in the study of 2-butenal adsorption on $SrTiO_3$ nanoparticle assigned the

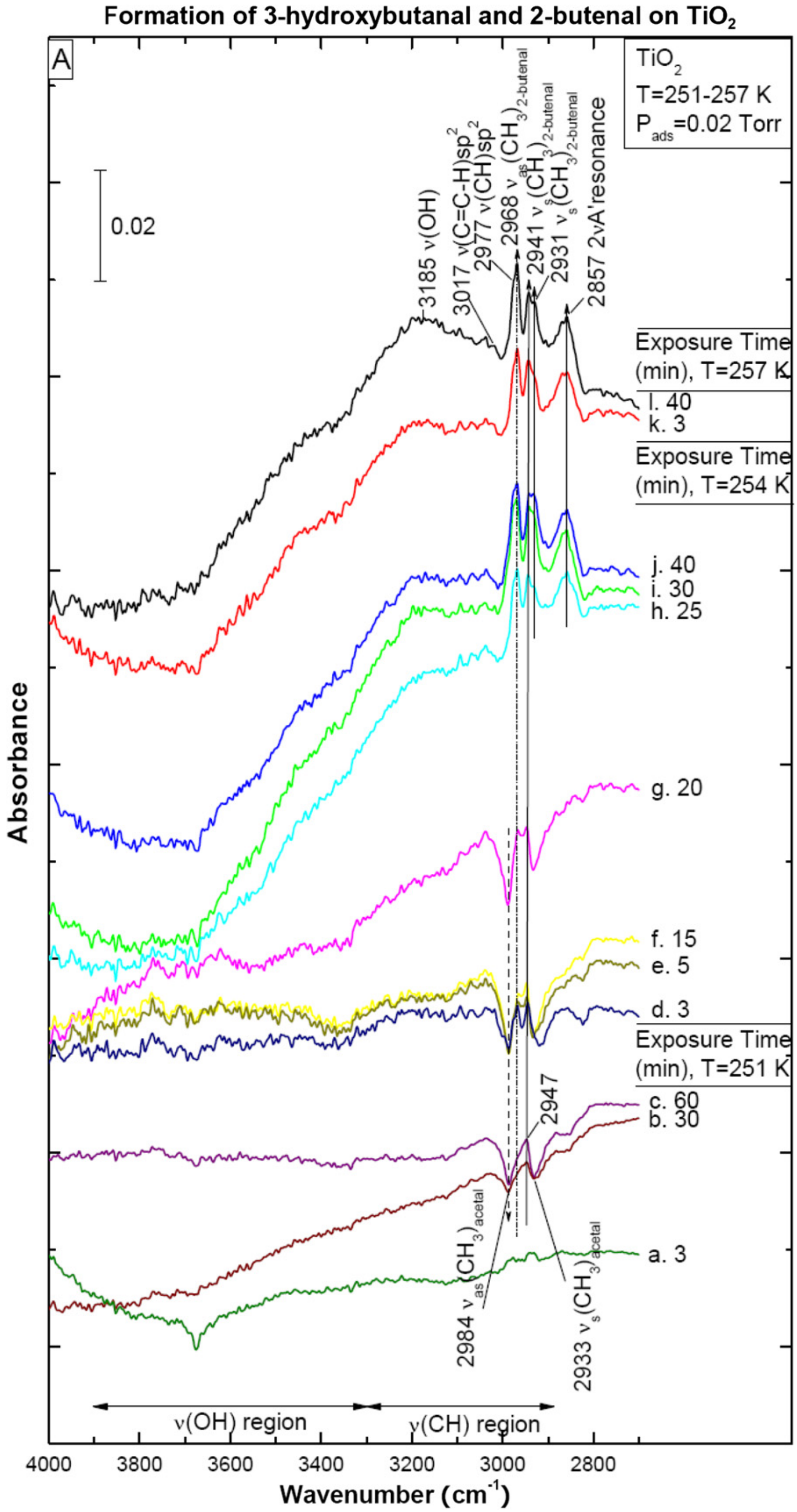

Fig. 2. Both time and temperature dependent subtracted infrared spectra (A—υ(CH) and υ(OH) regions and B—fingerprint region) of acetaldehyde on TiO_2 during gradual warming up at 251, 254, and 257 K, showing the formation of 3-hydroxybutanal and 2-butenal (spectra (a)–(c) at 251 K, spectra (d)–(j) at 254 K, spectra (k)–(l) at 257 K). The background used for subtraction is the spectrum shown in Figs. 1A and 1B (e).

peak at 1333 cm^{-1} for δ(CH) aldol. The peak at 1148 cm^{-1} can be assigned to ν(C–C) of 2-butenal, whereas the peak increasing in its intensity moderately at 1105 cm^{-1} is assignable to ν(C–C) and δ(COH) of aldol [42].

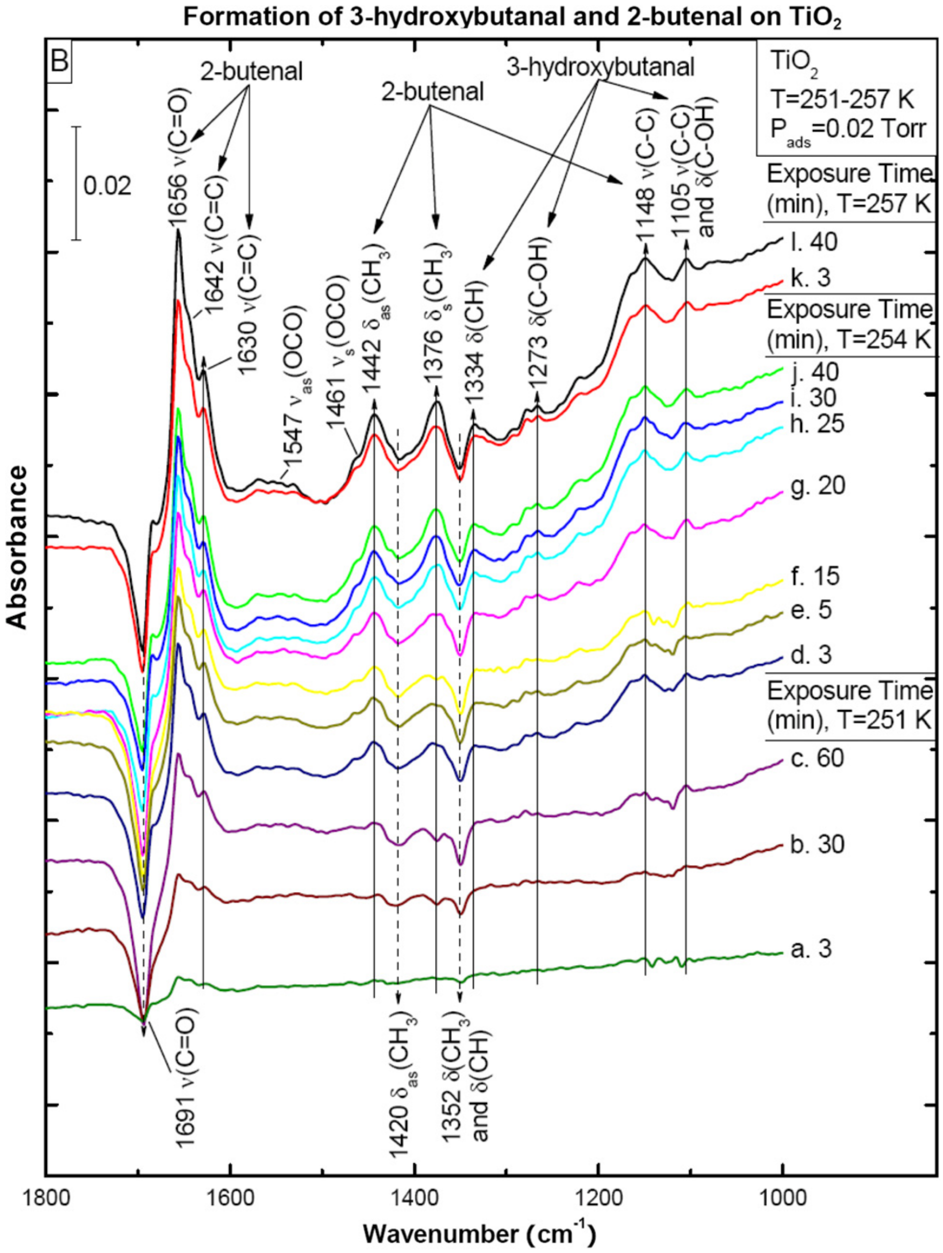

Fig. 2. (*continued*)

The weak feature developed at 1547 cm^{-1} along with a shoulder at 1461 cm^{-1} can be attributed to $\nu_{\text{as}}(\text{OCO})$ and $\nu_{\text{s}}(\text{OCO})$, respectively, for unidentate acetate species (because $\nu_{\text{as}}(\text{OCO}) - \nu_{\text{s}}(\text{OCO}) = 86\ \text{cm}^{-1} < 140\ \text{cm}^{-1}$). The formation of acetate species probably derived from the oxidation of acetaldehyde surface species as has been found in several previous studies on several metal oxide species including TiO_2, ZnO and CeO_2 [45–47].

For further confirmation of the assignment for surface species, two separate adsorption experiments using pure 3-hydroxybutanal and 2-butenal were carried out over the TiO_2 surface as shown in Fig. 3. Here the bottom spectrum (Figs. 3A and 3B (a)) is a redrawn infrared spectrum (shown in Figs. 1A and 1B (l)) obtained upon warming of adsorbed acetaldehyde to 257 K. The spectra (b) and (c) of Figs. 3A and 3B were obtained upon adsorption of pure 3-hydroxybutanal and 2-butenal, respectively. By comparing the spectrum (b) of 3-hydroxybutanal and (a), it is observed that the position and shape of the key infrared modes of $\upsilon(>\text{C}{=}\text{O})$, $\upsilon(\text{OH})$, and $\delta(\text{C–OH})$ appeared at 1658, 3187/3237 and 1273 cm^{-1} respectively, are similar. In addition, the peaks at 1334 and 1105 cm^{-1} assigned to $\delta(\text{C–H})$ aldol and $\delta(\text{C–OH})/\upsilon(\text{C–C})$ modes respectively, are also comparable. Thus it is plausible that acetaldehyde (spectrum (a)) undergoes aldol condensation forming 3-hydroxybutanal (spectrum (b)) which upon dehydration forms 2-butenal (spectrum (c)). The striking similarity in the peak position and intensity for $\upsilon(\text{C}{=}\text{C})$ modes at 1642 and 1629 cm^{-1} observed in both the aldol (spectrum (a)) and the 2-butenal (spectrum (b)) can be explained by considering the unstable nature 3-hydroxybutanal, which undergoes dehydration forming 2-butenal in contact with dehydrated and calcined TiO_2.

Fig. 4 shows the plot of normalized integrated absorbance of key infrared modes of reactant (acetaldehyde) and products (3-hydroxybutanal and 2-butenal) as a function of time and temperature. The integrated absorbance data for the plot were taken from the integrated area of infrared spectra collected for different time periods (shown in Figs. 2A and 2B) at different temperatures. Here the mode used for kinetic data for the disappearance of

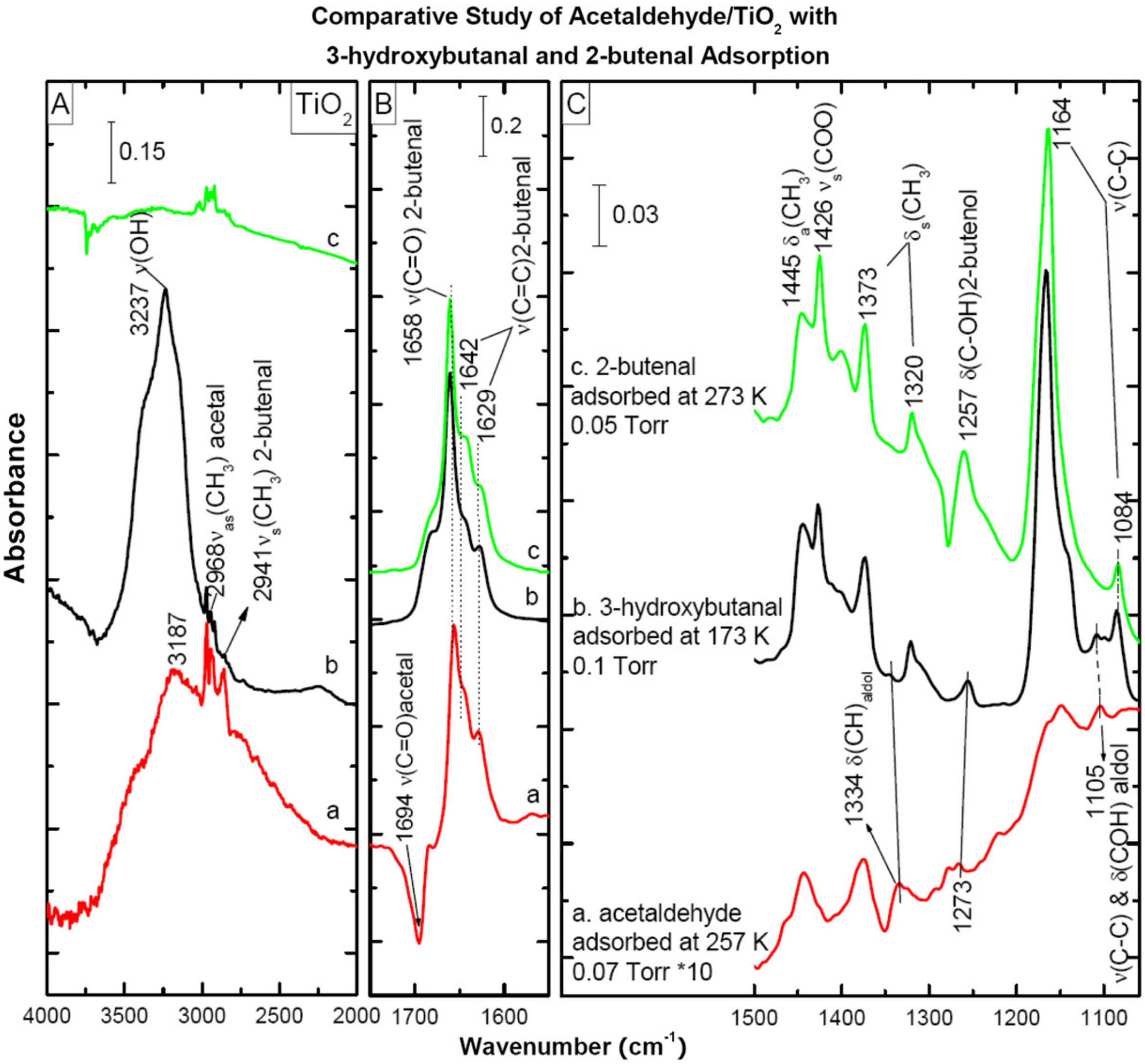

Fig. 3. Infrared spectra of adsorbed acetaldehyde (warmed to 257 K) compared to adsorption of 3-hydroxybutanal and 2-butenal adsorption. (Spectrum (a) adsorbed acetaldehyde warmed up to 257 K, spectrum (b) 3-hydroxybutanal adsorption at 173 K, spectrum (c) 2-butenal adsorption at 173 K.)

adsorbed acetaldehyde was $\upsilon(C{=}O)$ at 1691 cm^{-1}, whereas for aldol formation the well resolved modes for $\delta(CH)$aldol—1334 cm^{-1}, $\delta(C–OH)$—1273 cm^{-1} and $\delta(C–OH)/\upsilon(C–C)$ mode at 1105 cm^{-1} were used. The decrease in intensity of acetaldehyde corresponds to the formation of 2-butenal which was plotted by using the absorbance of unresolved $\upsilon(C{=}O)$ and $\upsilon(C{=}C)$ modes at 1656 and 1642 cm^{-1}. From the infrared spectra shown in Figs. 2A, 2B, the minimum temperature at which aldol condensation takes place is 251 K and approximately half of adsorbed acetaldehyde underwent the condensation reaction within 50 min. In addition, the formation of 3-hydroxybutanal is maximum at 251 K and the surface coverage slowly decreases as the temperature is raised to 257 K forming 2-butenal. Ultimately at higher temperature 3-hydroxybutanal surfaces species is so reactive that it undergoes fast dehydration on the surface forming 2-butenal and thus aldol surface species could not be detected.

3.3. *Proposed mechanisms for aldol condensation reaction of acetaldehyde on TiO_2 surface*

Fig. 5 shows the proposed mechanism of aldol condensation of acetaldehyde on TiO_2 surface. As acetaldehyde is introduced on the surface, a fraction of acetaldehyde is adsorbed through H-bonding with surface hydroxyl groups as identified by the depletion of two well-defined peaks at 3718 and 3651 cm^{-1} (Fig. 2A) [45–47]. When the temperature was raised to 251 K, the surface species ($H_2C–CH{=}O$) attacks the carbonyl group of another adsorbed acetaldehyde molecule which in turn abstracts a proton (H^+) from the Brönsted acid sites (Ti–OH–Ti), yielding 3-hydroxybutanal. This finding could be explained by the observation of continual depletion of an IR band at 1691 cm^{-1} (for $\nu(C{=}O)$ of acetaldehyde), with simultaneous formation of a strong feature at 1656 cm^{-1} which is assigned to $\nu(C{=}O)$ for both 3-hydroxybutanal and 2-butenal (shown in Fig. 2B). In addition, the weak feature at 1273 cm^{-1} for $\delta(C–O–H)$ in-plane bending along with well resolved weak bands at 1148 and 1105 cm^{-1} assigned to $\nu(C–C)$ and $\delta(C–O–H)$, respectively, for aldol surface species. This view is in consistent with the observation of gradual depletion of intensity of the $\delta(CH_3)$ mode of adsorbed aldehyde and concomitant formation of $\delta_{as}(CH_3)$, $\delta_s(CH_3)$ and $\delta(CH)$ald modes at 1442, 1376 and 1334 cm^{-1} for 2-butenal and aldol surface species. Finally the 3-hydroxybutanal molecules lose water to produce 2-butenal. The water molecules thus preferentially adsorb onto exposed Ti sites. The broad band at $\sim$3400 cm^{-1} and the distinct band 3185 cm^{-1} (Fig. 2A) might be due to the formation of water and 3-hydroxybutanal, respectively. Idriss et al. [7,8] investigated the reaction of acetaldehyde on both powder and single crystal TiO_2 surface and they found that the aldolization of acetaldehyde to 2-

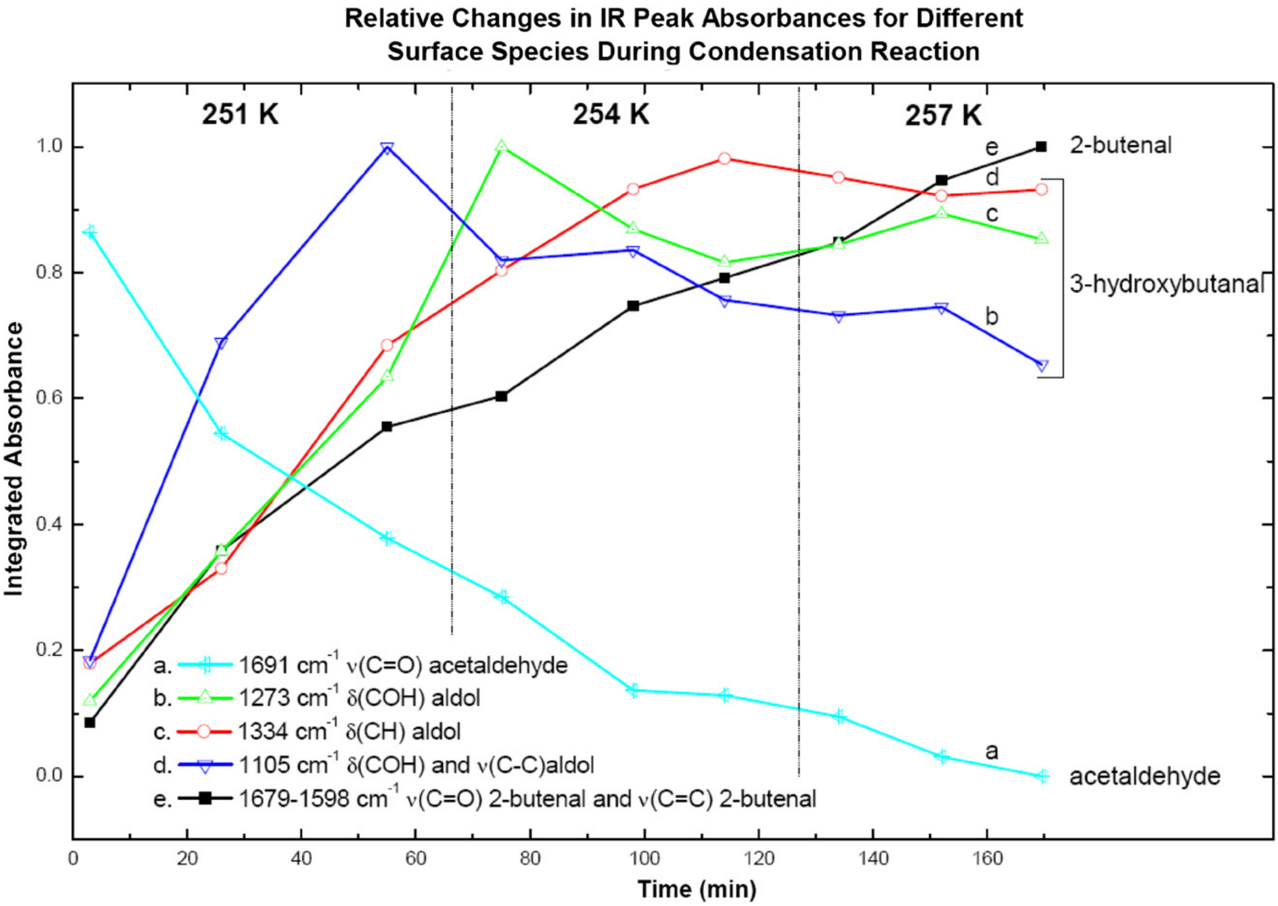

Fig. 4. Normalized integrated absorbance of selected infrared spectra bands, showing the onset of a condensation reaction of 3-hydroxybutanal and 2-butenal over TiO_2 during aldol condensation reaction of acetaldehyde (integrated spectra: (a) υ(C=O) acetaldehyde at 1691 cm^{-1}; (b) δ(COH) 3-hydroxybutanal at 1273 cm^{-1}; (c) δ(CH) 3-hydroxybutanal at 1334 cm^{-1}; (d) δ(COH) and υ(C–C) 3-hydroxybutanal at 1105 cm^{-1}; (e) υ(C=O) and υ(C=C) 2-butenal at 1679–1598 cm^{-1}).

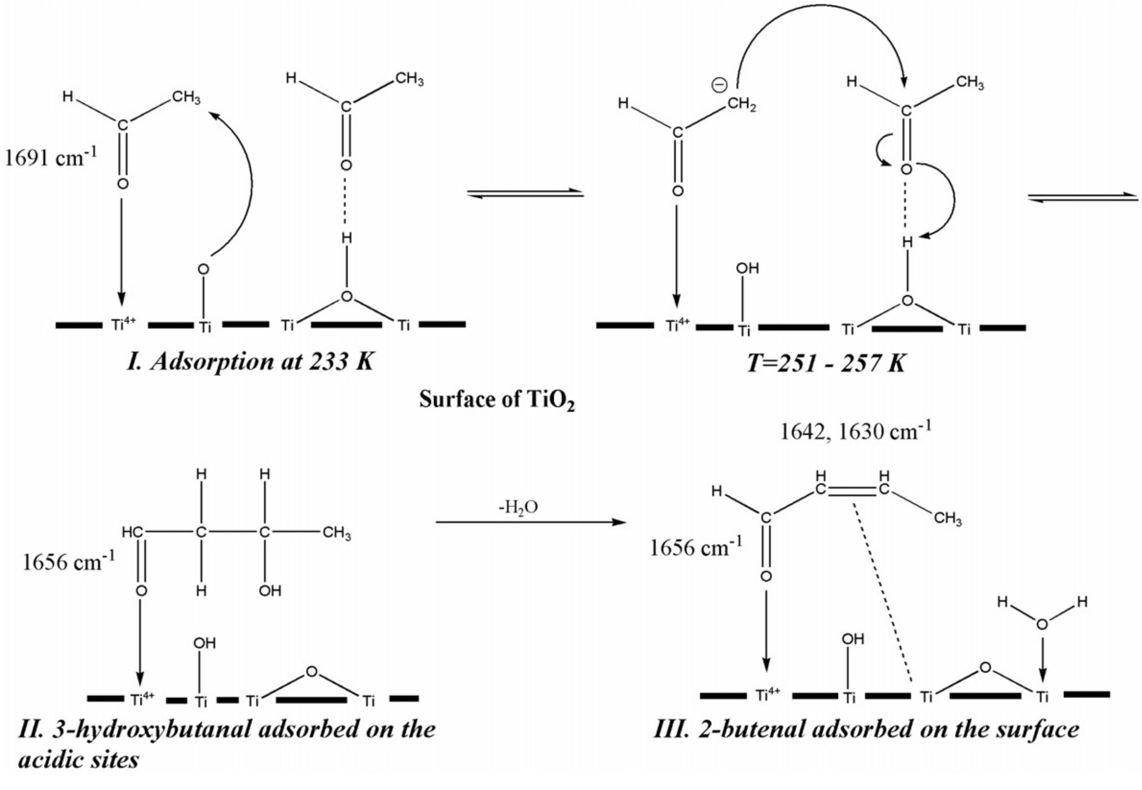

Fig. 5. Schematic of mechanism aldol condensation of acetaldehyde on TiO_2 surface.

butenal takes place because of the presence of oxide anions on the surface acting as Lewis base sites to abstract the α-hydrogen from the acetaldehyde. Rekoske and Barteau [12] investigated that the formation of 2-butenal upon the exposure of oxidized rutile TiO_2 to acetaldehyde occurred at higher than 373 K, but did not find IR spectra evidence for 2-butenal formation at low temperature. However, in this study, the reaction intermediate is identified on the surface at 251 K. At temperature below 251 K, no aldol condensation is observed on the surface, whereas as the temperature is raised to 273 K, the equilibrium shifted toward the final product of the reaction. Therefore, at relatively higher temperature, 3-hydroxybutanal is hardly detectable on the surface.

4. Conclusion

Acetaldehyde adsorbs onto TiO_2 in the temperature range of 233 to 250 K through H-bonding as well as through Lewis acid sites available on the surface. However, initiation of aldol condensation begins at 251 K, forming 3-hydroxybutanal intermediate which is characterized by distinct infrared features at 3185 cm^{-1} for ν(OH), 1334 cm^{-1} for δ(CH), 1273 cm^{-1} for δ(COH), and 1105 cm^{-1} for ν(C–C) and δ(COH) mode. The mechanism of condensation reaction involves initial abstraction of hydrogen atom from the α-carbon of aldehyde by Brönsted base sites forming a carbanion ($-CH_2CHO$), which in turn reacts with a second aldehyde molecule forming 3-hydroxybutanal. Direct comparison of experiments with pure 3-hydroxybutanal/TiO_2 also confirms the formation of 3-hydroxybutanal surface intermediate. Upon further warming, adsorbed aldol undergoes dehydration producing 2-butenal, and the identification of surface intermediate, 3-hydroxybutanal, is hardly discernible at or above 273 K.

Acknowledgments

We thank Office of the Naval Research and Center for Nanocomposites and Multifunctional Materials (CNCMM) for support of this work. We gratefully acknowledge with thanks the partial support of this work by NSF and DOD Multidisciplinary University Research Initiative (MURI) program administered by the Army Research Office. We also thank Prof. Khamis Siam for helpful discussions on B3LYP calculations of 3-hydroxybutanal.

References

[1] S. Zhang, Z.A. Munir, J. Mater. Sci. 27 (1992) 5789.
[2] H. Kominami, M. Kohno, Y. Kera, J. Mater. Chem. 10 (2000) 1151.
[3] K.Y. Song, M.K. Park, Y.T. Kwon, H.W. Lee, W.J. Chung, W.I. Lee, Chem. Mater. 13 (7) (2001) 2349–2355.
[4] S. Eibl, B.C. Gates, H. Knozinger, Langmuir 17 (1) (2001) 107–115.
[5] A. Linsebigler, G. Lu, J.T. Yates Jr., Chem. Rev. 95 (1995) 735–758.
[6] A. Fujishima, K. Honda, Nature 238 (1972) 37.
[7] H. Idriss, K. Kim, M. Barteau, J. Catal. 139 (1993) 119.
[8] H. Idriss, M.A. Barteau, Catal. Lett. 40 (1996) 147.
[9] A. Corma, V. Fornes, R.M. Martin-Aranda, H. Garcia, J. Primo, Appl. Catal. 59 (2) (1990) 237–248.
[10] P. Claus, Top. Catal. 5 (1–4) (1998) 51–62.
[11] J. Rasko, T. Kecskes, J. Kiss, Appl. Catal. A: Gen. 287 (2005) 244–251.
[12] J.E. Rekoske, M.A. Barteau, Langmuir 15 (1999) 2061.
[13] H. Swift, J.E. Bozik, F.E. Massoth, J. Catal. 15 (1969) 407.
[14] H. Idriss, C. Diagne, J.P. Hindermann, A. Kiennemann, M.A. Barteau, J. Catal. 155 (1995) 219.
[15] T.H. Ballinger, J.C.S. Wong, J.T. Yates Jr., Langmuir 8 (1992) 1676.
[16] P. Basu, T.H. Ballinger, J.T. Yates Jr., Rev. Sci. Instrum. 59 (8) (1988) 1321–1327.
[17] M.J. Frisch, G.W. Trucks, H.B. Schlegel, G.E. Scuseria, M.A. Robb, J.R. Cheeseman, J.A. Montgomery Jr., T. Vreven, K.N. Kudin, J.C. Burant, J.M. Millam, S.S. Iyengar, J. Tomasi, V. Barone, B. Mennucci, M. Cossi, G. Scalmani, N. Rega, G.A. Petersson, H. Nakatsuji, M. Hada, M. Ehara, K. Toyota, R. Fukuda, J. Hasegawa, M. Ishida, T. Nakajima, Y. Honda, O. Kitao, H. Nakai, M. Klene, X. Li, J.E. Knox, H.P. Hratchian, J.B. Cross, V. Bakken, C. Adamo, J. Jaramillo, R. Gomperts, R.E. Stratmann, O. Yazyev, A.J. Austin, R. Cammi, C. Pomelli, J.W. Ochterski, P.Y. Ayala, K. Morokuma, G.A. Voth, P. Salvador, J.J. Dannenberg, V.G. Zakrzewski, S. Dapprich, A.D. Daniels, M.C. Strain, O. Farkas, D.K. Malick, A.D. Rabuck, K. Raghavachari, J.B. Foresman, J.V. Ortiz, Q. Cui, A.G. Baboul, S. Clifford, J. Cioslowski, B.B. Stefanov, G. Liu, A. Liashenko, P. Piskorz, I. Komaromi, R.L. Martin, D.J. Fox, T. Keith, M.A. Al-Laham, C.Y. Peng, A. Nanayakkara, M. Challacombe, P.M.W. Gill, B. Johnson, W. Chen, M.W. Wong, C. Gonzalez, J.A. Pople, Gaussian 03, Revision C.02, Gaussian, Inc., Wallingford, CT, 2004.
[18] GaussView, Version 4.1, Roy Dennington II, Todd Keith and John Millam, Semichem, Inc., Shawnee Mission, KS, 2007.
[19] G. Rauhut, P. Pulay, J. Phys. Chem. 99 (1995) 3093–3100.
[20] P. Pulay, W. Meyer, Mol. Phys. 27 (2) (1974) 473–490.
[21] C.E. Blom, C. Altona, Mol. Phys. 31 (5) (1976) 1377–1391.
[22] P. Pulay, W. Meyer, J. Mol. Spectrosc. 40 (1971) 59–70.
[23] L. Zhao, Chem. Phys. Lett. 414 (2005) 28–33.
[24] L. Zhao, Chem. Phys. Lett. 431 (2006) 56–61.
[25] Y. Yamaguchi, H.F. Schaefer, J. Chem. Phys. 73 (1980) 2310.
[26] A.A. Davydov, Infrared Spectroscopy of Adsorbed Species on the Surface of Transition Metal Oxides, Wiley, Chichester, 1984, p. 38.
[27] A.A. Tsyganenko, V.N. Filimonov, J. Mol. Struct. 19 (1973) 579.
[28] A.A. Tsyganenko, V.N. Filimonov, Dokl. Akad. Nauk SSSR 203 (1972) 636.
[29] H. Knözinger, P. Ratnasamy, Catal. Rev. Sci. Eng. 17 (1978) 31.
[30] H.-P. Boehm, H. Knözinger, in: J.R. Anderson, M. Boudart (Eds.), Catalysis: Science and Technology, vol. 4, Springer, Berlin, 1983, p. 39.
[31] C.-A. Chang, B. Ray, D.K. Paul, D. Demydov, K.J. Klabunde, J. Mol. Catal. A Chem. 281 (2008) 99.
[32] Z. Yu, S.C. Chuang, J. Catal. 246 (2007) 118.
[33] H. Madhavaram, H. Idriss, J. Catal. 224 (2004) 358.
[34] D.K. Paul, C.D. Marten, J.T. Yates Jr., Langmuir 15 (1999) 4508.
[35] D. Panayotov, J.T. Yates, J. Phys. Chem. B 107 (38) (2003) 10560–10564.
[36] Z. Liu, J. Tabora, R.J. Davis, J. Catal. 149 (1994) 117.
[37] H. Hollenstein, Hs.H. Gunthard, Spectrochim. Acta 27 (1971) 2027.
[38] H.J. Oelichmann, D. Bougeard, B. Schrader, J. Mol. Struct. 77 (1981) 179.
[39] R.P. Young, N. Sheppard, J. Catal. 7 (1967) 223.
[40] J.C. Jesus, F. Zaera, Surf. Sci. 430 (1999) 99.
[41] A. Yee, S.J. Morrison, H. Idriss, J. Catal. 186 (1999) 279.
[42] W.-C. Wu, S.-J. Yang, C.-H. Ho, Y.-S. Lin, L.-F. Liao, J.-L. Lin, J. Phys. Chem. B 110 (19) (2006) 9627–9631.
[43] A.J. Barnes, H.E. Hallam, Trans. Faraday Soc. 66 (1970) 1932.
[44] J.H.S. Green, Trans. Faraday Soc. 59 (1963) 1559.
[45] R.N. Spitz, J.E. Barton, M.A. Barteau, M.A. Staley, A.W. Sleight, J. Phys. Chem. B 90 (1986) 4067.
[46] J. Boaventura, Ph.D. thesis, University of Delaware, 1989.
[47] A.A. El-Azhary, R.H. Hilal, Spectrochim. Acta 53 (1997) 1365.